Structures of hydrogen-bonded clusters of benzyl alcohol with water investigated by infrared-ultraviolet double resonance spectroscopy in supersonic jet

Nikhil Guchhait, Takayuki Ebata, and Naohiko Mikami

Citation: The Journal of Chemical Physics **111**, 8438 (1999); doi: 10.1063/1.480184
View online: http://dx.doi.org/10.1063/1.480184
View Table of Contents: http://scitation.aip.org/content/aip/journal/jcp/111/18?ver=pdfcov
Published by the AIP Publishing

Structures of hydrogen-bonded clusters of benzyl alcohol with water investigated by infrared-ultraviolet double resonance spectroscopy in supersonic jet

Nikhil Guchhait, Takayuki Ebata,[a),b)] and Naohiko Mikami[a)]
Department of Chemistry, Graduate School of Science, Tohoku University, Sendai 980-8578, Japan

(Received 5 April 1999; accepted 16 August 1999)

The structures of the benzyl alcohol and its hydrogen-bonded clusters with water have been investigated by infrared-ultraviolet double resonance vibrational spectroscopy along with *ab initio* molecular-orbital calculations. Characteristic shifts of the OH stretching vibrations of the benzyl alcohol site as well as the water sites were found, which are quite useful to determine the cluster structures. For bare benzyl alcohol, a planar conformer having no intramolecular hydrogen bond is dominant in the jet. On the other hand, the dominant species becomes a *gauche*-type conformer in the benzyl alcohol–$(H_2O)_n$ $(n=1-4)$ hydrogen-bonded clusters. In these clusters, the π-hydrogen bond between the phenyl plane and the OH group of the water cluster site is possible. Detailed intermolecular hydrogen bonding structures are discussed by comparing the observed spectra with the simulated spectra obtained by *ab initio* calculations. © *1999 American Institute of Physics.* [S0021-9606(99)01142-3]

I. INTRODUCTION

Molecular clusters are fascinating systems in the sense that they provide microscopic models for molecular level understanding of the photophysical and chemical properties of condensed phases.[1–3] Especially, hydrogen-bonded clusters are of special interest as their binding nature is inherently related to acidity, basicity, proton (hydrogen) transfer, and many other phenomena. Studies on the structure of the clusters involving water may be most important to reveal the microscopic properties of aqueous solutions and biological environments. Many properties of water arise from its special ability to form large hydrogen-bond networks in which individual molecule acts simultaneously as a hydrogen donor and an acceptor.

Recent spectroscopic studies on the gas phase clusters involving water molecules have brought a new insight in our understanding of the structures, energetics, and dynamics of their hydrogen bond networks. Rotational and vibrational spectroscopic measurements in microwave,[4–7] near-infrared,[8] and far-infrared[9–13] regions are quite useful for the characterization of their geometrical structures and the tunneling dynamics of hydrogen atom(s). It has been well established that the water dimer has a linear *trans* structure, while recent studies on the water trimer, tetramer, and pentamer by terahertz laser vibration-rotation tunneling spectroscopy proposed that these clusters have quasiplanar monocyclic ring structures, whereas the water hexamer has a cage structure.[14–17] In general, the smaller size clusters favor simple cyclic structures, while the larger ones prefer three-dimensional icelike structures. Numerous theoretical studies employing *ab initio* quantum chemical calculations and dynamical simulations have been done to elucidate the nature of water clusters.[18–26] However, several possible structures are often obtained as low lying conformers, and their relative energies sensitively differ for different basis sets, leading to the ambiguity to determine which structure is actually observed experimentally.

Up to now, various spectroscopic methods have been applied to reveal the structures and dynamics of the hydrogen-bonded clusters of aromatic compounds.[27–37] Among many spectroscopic works, vibrational spectroscopy of the OH stretching vibration is particularly important to analyze their structures, because the OH stretching vibration is a sensitive probe of the hydrogen-bond structure. Vibrational spectroscopy of the OH stretching vibrations for the size-selected clusters has become possible by using IR-UV double resonance spectroscopy. Our group used this spectroscopy to observe of the OH stretching vibrations of size-selected hydrogen bonded clusters of phenol, 2-naphthol, and tropolone.[38–41] It was found that in these clusters water molecules easily form hydrogen-bonded networks involving the OH group of the aromatic molecules. It was shown that small size clusters exhibit a planar ring type structure while larger size clusters tend to form three-dimensional icelike structure. Zwier's group also observed the similar size dependence of the structure of water cluster in the benzene–$(H_2O)_n$ system.[42–45]

In this paper, we report our investigation of the structures of benzyl alcohol–$(H_2O)_n$. The interesting point in this system is that the bare molecule has an ability of forming intramolecular hydrogen bond between alcoholic OH and the π-electrons of the phenyl ring. Benzyl alcohol (BzA) is of particular interest in its versatile synthetic utility and in its role in the natural products.[46–49] Since BzA is known to be a flexible molecule, many conformers are possible associated with the rotation of the C–C bond as described below. One

a)Authors to whom correspondence should be addressed.
b)Electronic mail: ebata@qclhp.chem.tohoku.ac.jp

of our goals of the present spectroscopic investigation is to solve the longstanding structural ambiguity for BzA. In our previous paper, we reported the observation of the OH stretching vibrations of BzA and its homologs by infrared(IR)-ultraviolet(UV) double resonance spectroscopy in supersonic jets.[50] For bare BzA, we found two isomers whose OH stretching vibrational frequencies are different with each other. We assigned one of the two species to the planar conformer and the other to the *gauche* conformer, and reported that the planar conformer is dominant in the jet-cooled condition.

In this study, we extend the work to the determination of the structures of BzA–$(H_2O)_n$ hydrogen-bonded clusters. We applied the IR-UV double resonance spectroscopy to observe the IR spectra of size-specified BzA–$(H_2O)_n$. The IR spectra of the OH stretching bands of not only the BzA site but also of the water site were measured. In parallel with the spectroscopic measurements, we have carried out *ab initio* calculations to predict the structures of the clusters. By comparing the observed spectrum with the simulated ones for the energy-optimized conformers, we determined the most probable structure which reproduce the observed IR spectrum. It was found that though the dominant conformer is the planar form in the monomer, the *gauche* conformer becomes dominant in the BzA–$(H_2O)_n$ clusters.

II. EXPERIMENT

The details of the experimental setup were described elsewhere.[50] The jet-cooled molecules were generated by a supersonic expansion of a gaseous mixture of the sample heated at 330 K and helium into vacuum through a pulsed nozzle. For the measurement of the laser induced fluorescence (LIF) spectra, the jet-cooled molecules were excited with the UV light generated by a second harmonic of a XeCl excimer laser pumped dye laser (Lambda Physik LPX 100 FL 2002). The total fluorescence was detected by a photomultiplier tube (Hamamatsu Photonics IP 28). The output signal was processed by a boxcar integrator (PAR 4420) controlled by a personal computer.

IR-UV double resonance spectroscopy with fluorescence detection, so called fluorescence detected infrared (FDIR) spectroscopy, for the jet-cooled molecules utilizes the population labeling technique to measure the IR spectrum of selectively chosen species with the UV laser light. The ground state population of a particular species in the jet was monitored by the S_1-S_0 fluorescence intensity with the UV light. A tunable IR pulse was introduced at ~50 ns prior to the UV pulse. When the IR frequency is resonant with the vibrational transition of the species, the ground state population is reduced, resulting in a depletion of the fluorescence signal. Thus, by scanning the IR wavelength while monitoring the fluorescence signal, the fluorescence-dip spectrum, that is, the fluorescence detected IR spectrum (FDIRS), is obtained. The tunable IR light was generated with a $LiNbO_3$ crystal by a difference frequency mixing between a part of the second harmonic of a Nd:YAG laser (Quanta Ray GCR 230) and the output of the Nd:YAG laser pumped dye laser (Continuum ND-6000). The angle of the crystal was controlled by an autotracking system (Inrad autotracker III). The tunable IR output passed through a CaF_2 Brewster-angle window and filters to eliminate the visible laser light. The UV and IR beams were introduced into the vacuum chamber in a counter propagating manner and were focused by lenses ($f=250$ mm for IR and $f=500$ mm for UV) on the supersonic jet. Fluorescence was detected by a photomultiplier tube and the photocurrent was processed by the same boxcar integrator described above.

Benzyl alcohol was purchased from Aldrich Chemical Co. and was used without further purification. *Ab initio* molecular orbital calculations for obtaining stable conformers of BzA–$(H_2O)_n$ were done with the GAUSSIAN 94 program at the HF/6-31G and HF/6-31G(d,p) levels.[51] Calculated parameters are presented in the discussion section of this paper as a tabulated form. The determinations of the cluster structures were carried out by comparing the observed spectra with those of the simulated ones for the energy-optimized structure.

III. RESULTS AND DISCUSSION

A. Bare benzyl alcohol

The conformational discrimination of the flexible molecule, such as rotamers of BzA, has been a long-standing problem. From many IR spectroscopic studies on a series of aryl alcohols (benzyl alcohol homologs) at room temperature, it is well established that the gauche conformer, that is the hydrogen-bonded conformer having a lower OH stretching frequency dominates the planar one, that is the nonhydrogen-bonded conformer having a higher OH stretching frequency.[52–54] *Ab initio* calculations of benzyl alcohol suggested that both the planar and the gauche forms are stable conformers.[55] However, empirical molecular force field calculations predicted only the planar form as the energy minimum conformer.[56] Very recently, Bernstein's group reported the mass-resolved resonance enhanced multiphoton ionization (REMPI) spectroscopic study of jet cooled BzA (Ref. 57) and emphasized that only the perpendicular conformer exists in the jet.

In our previous paper, we investigated the conformational discrimination of BzA by IR-UV double resonance spectroscopy.[50] Figure 1 shows the LIF spectra of (a) BzA, and (b) BzA–$(H_2O)_{n=1-4}$ hydrogen-bonded clusters in supersonic jets. The observed LIF spectrum of the bare molecule is very similar to the spectrum obtained by Bernstein's group.[57] However, we observed a new band B at 46 cm^{-1} lower frequency side of the strongest band A at 37 527 cm^{-1}. We confirmed that both bands A and B belong to bare BzA by measuring the mass-resolved REMPI spectrum, and then we measured the FDIR spectra by monitoring those bands.[50] Figure 2 shows the FDIR spectra obtained by monitoring the bands A and B, respectively, and corresponding structures of BzA obtained by *ab initio* calculation at the HF/6-31G level. As seen in the figure, the frequency of the OH stretch band for band A is 3650 cm^{-1}, and that for band B is 3585 cm^{-1}. The IR spectra observed by monitoring the bands marked by asterisks in Fig. 1(a) exhibit the OH band at the same frequency of 3650 cm^{-1}.[50] Thus, they originate from the same conformer, and the intense band A at 37 527 cm^{-1} is their

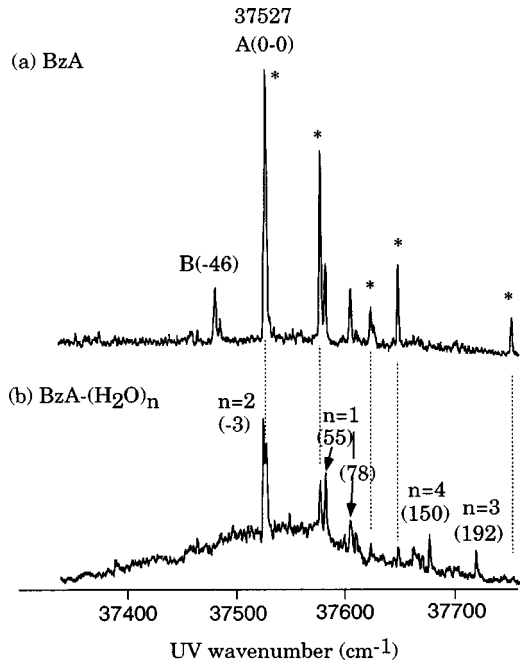

FIG. 1. Laser induced fluorescence (LIF) spectra of jet-cooled benzyl alcohol (BzA) and its clusters in the band origin region of the S_1-S_0 transition. (a) BzA with low water vapor pressure and (b) with higher water vapor pressure. The bands marked by asterisks belong to the same conformer of band *A* at 37 527 cm^{-1}.

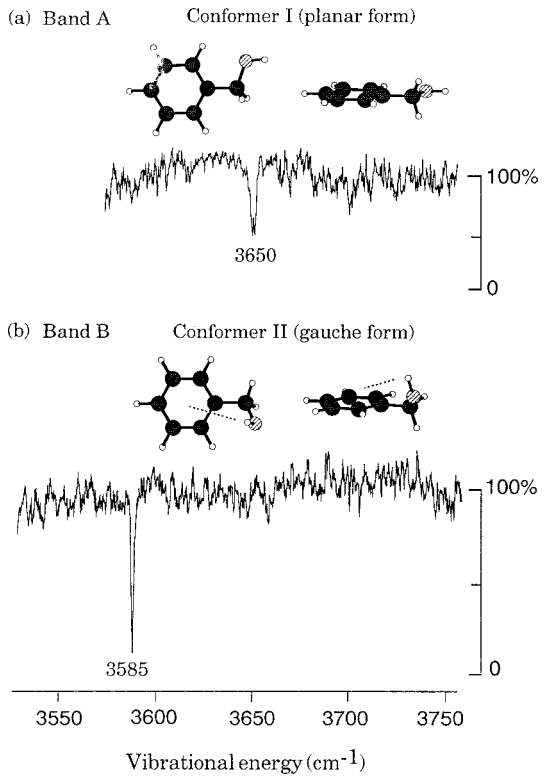

FIG. 2. Fluorescence detected infrared (FDIR) spectra of bare BzA observed by monitoring (a) band *A* and (b) band *B* of Fig. 1. Also shown are the corresponding structures of BzA calculated at the HF/6-31G level.

band origin, while the band *B* belongs to the different conformer. The observed IR frequencies are listed in Table I.

As shown in Fig. 2, Conformer I is the ''planar'' conformer whose alcoholic OH group is pointing to the opposite direction of the phenyl ring, and it has no chance to form intramolecular hydrogen bonding. On the other hand, Conformer II is the ''*gauche*'' form, which has a possibility of the intramolecular hydrogen bond between the alcoholic OH group and π-electrons of phenyl plane. Since the intramoleculer hydrogen bond reduces the alcoholic OH stretching vibrational frequency, we concluded that the species associated with band *B* corresponds to the ''*gauche*'' conformer, and the dominant species associated with band A to the nonhydrogen-bonded ''planar'' conformer.

B. Benzyl alcohol–(H_2O)

The LIF spectrum of BzA–$(H_2O)_n$ is shown in Fig. 1(b). The assignments of the bands with respect to the sizes are given by Li *et al.*[47] The bands at +55 and +78 cm^{-1} higher frequency side of band A of bare BzA are associated with BzA–H_2O. Figure 3(a) shows the FDIR spectrum for BzA–H_2O obtained by fixing the UV frequency to the +55 cm^{-1} band. We obtained the similar IR spectrum for the +78 cm^{-1} band, so that the two bands belong to the same species. Vibrational frequencies of the observed bands are also listed in Table I. The FDIR spectrum shows three distinct bands in the OH stretching region, and several bands in the CH stretching region. Bands in the 3000–3100 cm^{-1} region correspond to the aromatic CH stretching vibrations, while those below 3000 cm^{-1} are assigned as the aliphatic CH stretching vibrations.

Among the three OH stretch bands of the BzA–H_2O, one is due to BzA site and two to H_2O site. The intense lowest frequency band at 3568 cm^{-1} is assigned to the alcoholic OH stretch of the BzA site. This band is 82 cm^{-1} red-shifted from that of the planar form of bare BzA and 17 cm^{-1} from the *gauche* form. This frequency reduction is explained by that the alcoholic OH bond is weakened upon the σ-hydrogen bond formation with the oxygen of H_2O. The question as to whether BzA has a *gauche* or a planar structure in the cluster will be discussed later. The bands at 3622 and 3733 cm^{-1} are assigned to the symmetric and antisymmetric stretching vibrations of the H_2O site, respectively. The frequencies of the former and the latter vibrations are redshifted by 30 and 24 cm^{-1},[58] respectively, from those of the H_2O monomer. In addition, as seen in Fig. 3(a), it is noticed that the IR intensity of the symmetric stretch is comparable with that of the antisymmetric stretch. This intensity pattern is quite different from that of bare H_2O or phenol–H_2O, where two OH oscillators of H_2O are symmetrically equivalent.[38] Thus, the observed intensity pattern in the IR spectrum indicates that the two oscillators of H_2O are inequivalent with each other in the cluster.

The calculated structures of BzA–H_2O at the HF/6-31G(d,p) level are shown in Fig. 4, and the calculated frequencies, IR intensities, and energies are also listed in Table II. In Conformer I of Fig. 4, which is the minimum energy conformer at the HF/6-31G(d,p) level, BzA exhibits the *gauche* form and H_2O locates above the phenyl plane in such a way that a cyclic hydrogen bond network is formed. That is, the alcoholic OH group of BzA is hydrogen bonded

TABLE I. The frequencies of the observed vibrational bands (cm^{-1}), and the frequencies (cm^{-1}) and the IR intensities of the OH stretching vibrations obtained by *ab initio* calculation for benzyl alcohol (BzA) and benzyl alcohol–$(H_2O)_n$.

Cluster size	Observed frequencies	Intensities	Assignment	Calculated frequencies[a]	Assignment[b]
Bare BzA	3650	*s*	ν_{OH}	3651(29)	ν_{OH}(planar)
	3585	*vs*	ν_{OH}	3623(40)	ν_{OH}(gauche)
$n=1$	3733	*s*	$\nu_{OH}^{antisym.}$	3733(110)	$\nu_{OH}^{antisym.}$
	3622	*s*	$\nu_{OH}^{\pi\text{-bonded}}$	3633(36)	$\nu_{OH}^{sym.}$
	3608	*vw*			
	3593	*vw*			
	3568	*vs*	ν_{OH}	3596(228)	ν_{OH}
	3098	*s*	$\nu_{CH}^{aromatic}$		
	3077	*s*	$\nu_{CH}^{aromatic}$		
	3040	*s*	$\nu_{CH}^{aromatic}$		
	2951	*s*	$\nu_{CH}^{aliphatic}$		
$n=2$	3732	*s*			
	3725	*vs*	$\nu_{OH}^{antisym.}$	3718(75)	$\nu_{OH}^{antisym.}$
	3718	*s*	$\nu_{OH}^{antisym.}$	3715(115)	$\nu_{OH}^{antisym.}$
	3712	*w*			
	3705	*s*			
	3701	*w*			
	3595	*vs*	$\nu_{OH}^{\pi\text{-bonded}}$	3629(83)	$\nu_{OH}^{sym.}$
	3543	*m*	ν_{int}		
	3532	*w*	ν_{int}		
	3526	*w*	ν_{int}		
	3520	*m*	ν_{int}		
	3510	*s*	ν_{int}		
	3503	*vs*	ν_{OH}	3563(371)	ν_{OH}^{aym}, ν_{OH}
	3472	*w*	ν_{int}		
	3462	*vs*	ν_{OH}	3530(284)	$\nu_{OH}^{sym.}$, ν_{OH}
	3204	*m*	$2\nu_{OH}^{bend}$		
	3098	*m*	$\nu_{CH}^{aromatic}$		
	3078	*m*	$\nu_{CH}^{aromatic}$		
	3037	*m*	$\nu_{CH}^{aromatic}$		
	2939	*m*	$\nu_{CH}^{aliphatic}$		
$n=3$	3717	*s*	$\nu_{OH}^{antisym.}$	3711(132)	$\nu_{OH}^{antisym.}$
				3709(88)	$\nu_{OH}^{antisym.}$
	3661	*s*	$\nu_{OH}^{\pi\text{-bonded}}$	3689(115)	$\nu_{OH}^{antisym.}$
	3458	*vs*	ν_{OH}	3544(225)	$\nu_{OH}^{sym.}$, ν_{OH}
	3383	vs	ν_{OH}	3516(482)	$\nu_{OH}^{sym.}$, ν_{OH}
	3350	*vs*	ν_{OH}	3505(506)	$\nu_{OH}^{sym.}$, ν_{OH}
	3296	*m*	ν_{OH}	3457(117)	$\nu_{OH}^{sym.}$, ν_{OH}
	3208	*m*	$2\nu_{OH}^{bend}$		
	3099	*w*	$\nu_{CH}^{aromatic}$		
	3078	*m*	$\nu_{CH}^{aromatic}$		
	3047	*s*	$\nu_{CH}^{aromatic}$		
	2970	*s*	$\nu_{CH}^{aliphatic}$		
	2947	*m*	$\nu_{CH}^{aliphatic}$		
$n=4$	3724	*s*	$\nu_{OH}^{antisym.}$	3708(72)	$\nu_{OH}^{antisym.}$
	3717	*vs*	$\nu_{OH}^{antisym.}$	3706(119)	$\nu_{OH}^{antisym.}$
				3698(88)	$\nu_{OH}^{antisym.}$
	3653	*s*	$\nu_{OH}^{\pi\text{-bonded}}$	3691(195)	$\nu_{OH}^{antisym.}$
	3537	*vw*	?		
	3440	*vs*	ν_{OH}	3584(223)	$\nu_{OH}^{sym.}$, ν_{OH}
	3404	*s*	ν_{OH}	3565(244)	$\nu_{OH}^{sym.}$, ν_{OH}
	3328	*s*	ν_{OH}	3498(436)	$\nu_{OH}^{sym.}$, ν_{OH}
	3288	*s*	ν_{OH}	3467(809)	$\nu_{OH}^{sym.}$, ν_{OH}
				3412(323)	$\nu_{OH}^{sym.}$, ν_{OH}
	3198	*s*	$2\nu_{OH}^{bend}$		
	3099	*w*	$\nu_{CH}^{aromatic}$		
	3078	*s*	$\nu_{CH}^{aromatic}$		
	3046	*s*	$\nu_{CH}^{aromatic}$		
	2964	*s*	$\nu_{CH}^{aliphatic}$		
	2946	*m*	$\nu_{CH}^{aliphatic}$		

[a]Calculated frequencies are presented at (HF/6-31G) level for benzyl alcohol and at the HF/6-31G(d,p) level for benzyl alcohol–$(H_2O)_n$ clusters. Calculated OH frequencies are multiplied by a factor of 0.903 for benzyl alcohol and 0.8785 for benzyl alcohol–$(H_2O)_n$. IR intensities (km/mol) are shown in the parentheses.

[b]Assignments based on the vector models of the calculated normal modes. Usually symmetric OH modes of H_2O are coupled with the alcoholic OH mode.

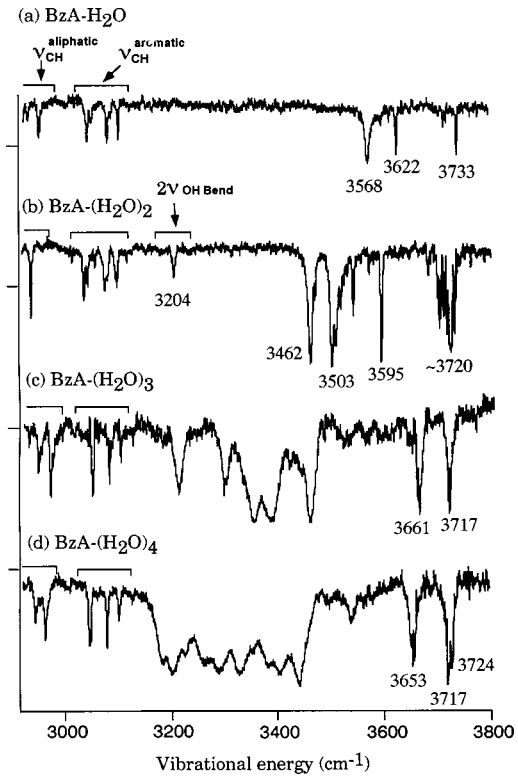

FIG. 3. FDIR spectra for the BzA–$(H_2O)_n$ clusters in the S_0 state. UV laser frequencies were fixed to the bands of (a) +55 cm^{-1} (BzA–H_2O), (b) −3 cm^{-1} (BzA–$(H_2O)_2$), (c) +192 cm^{-1} (BzA–$(H_2O)_3$), and (d) +150 cm^{-1} (BzA–$(H_2O)_4$) in the LIF spectrum of Fig. 1.

to the oxygen of H_2O, and the OH group of H_2O is hydrogen bonded to the π-electrons of phenyl plane. The other hydrogen atom of H_2O is free from the hydrogen bond. Thus, the environment of the three OH groups in Conformer I is quite different with each other. Conformer II is the planar form, which is 697 cm^{-1} higher in energy than Conformer I. In the planar conformer, the oxygen of H_2O is bound to the hydrogen of the alcoholic OH that lies in the same aromatic plane

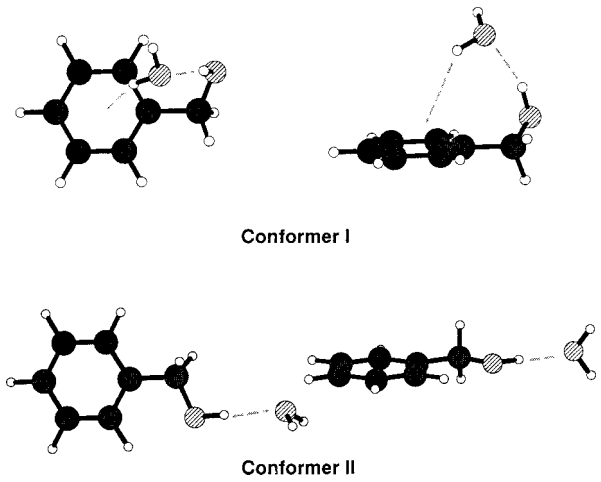

FIG. 4. Energy optimized structures for BzA–H_2O at the HF/6-31G(d,p) level. Conformer I (left: top view, right: side view) is minimum energy *gauche*-type conformer, Conformer II (left: top view, right: side view) is the planar type higher energy conformer. Possible hydrogen bondings are shown with broken lines.

of BzA. The conformer preserves the Cs symmetry and the two OH oscillators of H_2O are symmetrically equivalent. In this case, the IR intensity of the symmetric stretch becomes much weaker than that of the antisymmetric stretch, which have been demonstrated for phenol–H_2O and 2-naphthol-H_2O.[38,41]

The simulated spectra at the HF/6-31G(d,p) level for the two conformers of BzA–H_2O are shown in Fig. 5 to be compared with the observed FDIR spectrum. In Conformer I [Fig. 5(b)], the IR intensity of the symmetric stretch of H_2O is comparable to that of the antisymmetric stretch due to the hydrogen bond to the phenyl π-electrons. In the spectrum of Conformer II [Fig. 5(c)], on the other hand, the IR intensity of the symmetric stretch is very weak, which does not agree with the observed spectrum. Thus, the simulated spectrum of Conformer I agrees well with the observed IR spectrum and we conclude that BzA takes the ''*gauche*'' structure in BzA–H_2O.

C. Benzyl alcohol–$(H_2O)_2$

As shown in Fig. 1(b), the 0–0 band of the benzyl BzA–$(H_2O)_2$ is located at the 3 cm^{-1} lower frequency side of band A of bare BzA. This band was analyzed in detail by Li *et al.* from the mass-resolved REMPI spectra.[47] The FDIR spectrum obtained by monitoring the −3 cm^{-1} band is shown in Fig. 3(b). The bands below ~3100 cm^{-1} are assigned to the CH stretching vibrations. Among them, the aromatic CH stretch bands between 3000 and 3100 cm^{-1} are similar to those of BzA–H_2O, while the aliphatic CH stretch bands below 3000 cm^{-1} are slightly red-shifted, indicating that the CH_2 group is distorted. An isolated band at 3204 cm^{-1} is assigned to the overtone band of the OH bending mode of the H_2O site, similar to the case of phenol–$(H_2O)_3$.[38]

Though five bands are expected to appear in the OH stretching region for BzA–$(H_2O)_2$ originating from BzA and two H_2O molecules, the observed spectrum between 3400 and 3800 cm^{-1} in Fig. 3(b) exhibits much more bands with a complicated pattern. It was found the complexity of the spectrum of Fig. 3(b) is due to that the used IR power is so intense that even the weaker bands appeared with comparable intensities. We observed the OH stretching vibrational spectra of BzA–$(H_2O)_2$ at different IR powers, which are shown in Figs. 7(a)–7(c). As seen in the figures, the spectrum becomes simpler with the decrease of the IR laser power, and in Fig. 7(c) the bands are classified into four groups; the intense bands at 3462, 3503, and 3595 cm^{-1}, and congested band at 3695–3740 cm^{-1}. The former three bands are assigned to the hydrogen-bonded alcoholic OH stretching vibration of BzA and symmetric vibrations of two H_2O molecules. The satellite bands accompanied with the 3503 cm^{-1} band observed at a higher IR laser power [Fig. 7(a)], are thought to be the combination bands with intermolecular vibrations.

This situation is also the same for the bands in the 3695–3740 cm^{-1} energy region. More than six bands appeared close each other with comparable intensities in Fig. 7(a), though only two antisymmetric stretching vibrational bands

TABLE II. Calculated energies (cm^{-1}), frequencies (cm^{-1}), and intensities at the HF/6-31G(d,p) levels for OH modes of benzyl alcohol–$(H_2O)_n$ clusters.[a]

	Calculated IR frequencies[b] (intensities)[c]			
	Conformer I	Conformer II	Conformer III	Assignment
$n=1$				
$\Delta E(cm^{-1})$	0[d](0)[e]	+697(+523)		
	3733[f](110)[g]	3741(93)		$\nu_{OH}^{antisym.}$
	3633(36)	3641(10)		$\nu_{OH}^{sym.}$
	3596(228)	3610(503)		ν_{OH}
$n=2$				
$\Delta E(cm^{-1})$	0(0)	+2434(+3485)	+51(−526)	
	3718(75)	3738(69)	3716(118)	$\nu_{OH}^{antisym.}$
	3715(115)	3737(107)	3712(113)	$\nu_{OH}^{antisym.}$
	3629(83)	3641(30)	3571(445)	$\nu_{OH}^{sym.}$
	3563(371)	3635(26)	3569(461)	$\nu_{OH}^{sym.}$
	3530(284)	3599(246)	3531(32)	ν_{OH}
$n=3$				
$\Delta E(cm^{-1})$	0(0)	+1048(+2288)	not stable(+57)	
	3711(132)	3712(93)		$\nu_{OH}^{antisym.}$
	3709(88)	3704(84)		$\nu_{OH}^{antisym.}$
	3689(115)	3701(177)		$\nu_{OH}^{antisym.}$
	3544(225)	3609(99)		$\nu_{OH}^{sym.}, \nu_{OH}$
	3516(482)	3578(286)		$\nu_{OH}^{sym.}, \nu_{OH}$
	3505(506)	3538(385)		$\nu_{OH}^{sym.}, \nu_{OH}$
	3457(117)	3484(256)		$\nu_{OH}^{sym.}, \nu_{OH}$
$n=4$				
$\Delta E(cm^{-1})$	0(0)	+199(−34)		
	3708(72)	3710(93)		$\nu_{OH}^{antisym.}$
	3706(119)	3709(94)		$\nu_{OH}^{antisym.}$
	3698(88)	3695(123)		$\nu_{OH}^{antisym.}$
	3691(195)	3668(45)		$\nu_{OH}^{antisym.}$
	3584(223)	3636(317)		$\nu_{OH}^{sym.}, \nu_{OH}$
	3565(224)	3552(182)		$\nu_{OH}^{sym.}, \nu_{OH}$
	3498(436)	3525(368)		$\nu_{OH}^{sym.}, \nu_{OH}$
	3467(809)	3477(606)		$\nu_{OH}^{sym.}, \nu_{OH}$
	3412(323)	3431(190)		$\nu_{OH}^{sym.}, \nu_{OH}$

[a]All numbers are round up to the nearest number.
[b]Calculated frequencies are multiplied by a factor of 0.8785 for HF/6-31G(d,p) level.
[c]Numbers in the parentheses are calculated IR intensities.
[d]Relative energy with respect to Conformer I at the HF/6-31G(d,p) level.
[e]Relative energy with respect to Conformer I at the HF/6-31G level.
[f]Frequencies in cm^{-1}.
[g]IR intensities (km/mol).

due to two H_2O molecules should appear in this region. As seen in Fig. 7(c), however, only the bands at ~3724 cm^{-1} remain strong even under a weak IR laser power condition and they are assigned to the antisymmetric vibrations of the H_2O site. The other bands which observed at a higher IR laser power condition are thought to be the overtone or combination bands which appear by the anharmonic coupling with the antisymmetric bands of H_2O molecules, though the reason why the anharmonic coupling is so strong in BzA–$(H_2O)_2$ is not known.

Figure 6 shows three stable conformers of BzA–$(H_2O)_2$, which are energy optimized at the HF/6-31G(d,p) level. Calculated vibrational frequencies, IR intensities, and the energies are listed in Table II. Among them, Conformer I (*gauche* form cluster) is the minimum energy isomer at the HF/6-31G(d,p) level. In this conformer, a water dimer, $(H_2O)_2$, is hydrogen-bonded to the alcoholic OH as well as to the phenyl plane. Conformer II in Fig. 6 is an another *gauche* type BzA–$(H_2O)_2$ cluster. As seen in Table II, Conformer II is higher energy isomer than Conformer II. The structure is similar to the *gauche* BzA–H_2O cluster with an additional H_2O being hydrogen-bonded to the phenyl plane from the opposite side. Conformer III is the planar type isomer of BzA–$(H_2O)_2$, where two H_2O molecules and the alcoholic OH group form a ring structure and this structure is quite similar to those of phenol–$(H_2O)_2$ or 2-naphthol–$(H_2O)_2$. Although Conformer III is the minimum energy conformer at the HF/6-31G level, it becomes slightly higher in energy (+51 cm^{-1}) than the Conformer I at the HF/6-31G(d,p) level calculation. Thus, we are unable to determine the probable structure from the stabilization energy.

Figure 7 shows the comparison of the observed spectrum of the OH stretch bands with the simulated ones for the three

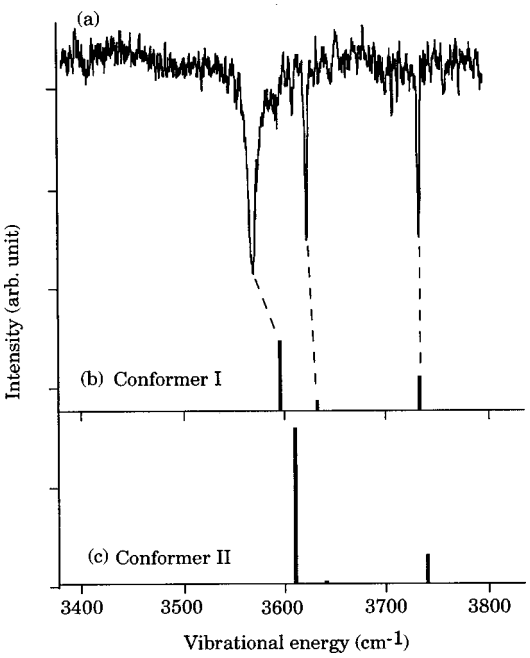

FIG. 5. Comparison of (a) the observed FDIR spectrum of the OH stretching bands of BzA–H_2O with the calculated spectra (stick diagram) for two conformers obtained at the HF/6-31G(d,p) level calculation; (b) Conformer I and (c) Conformer II. The vibrational frequencies are multiplied by a factor of 0.8785.

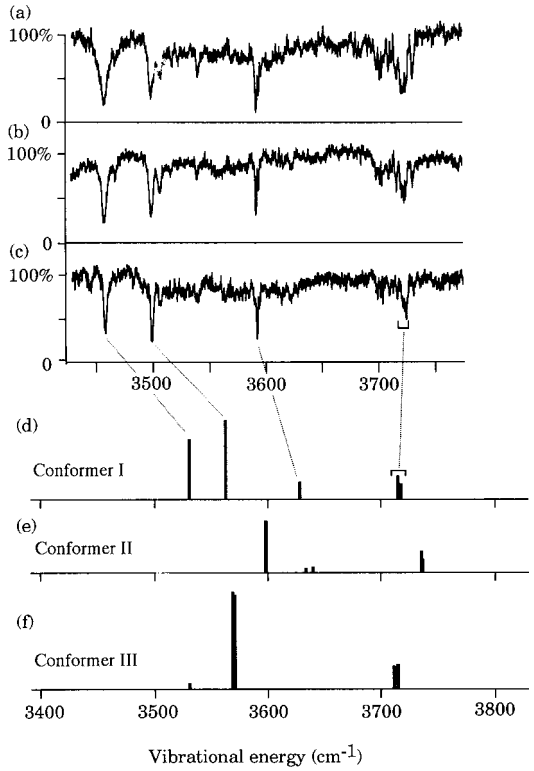

FIG. 7. (a)–(c) FDIR spectrum of the OH stretching vibrations of BzA–$(H_2O)_2$ measured at different IR laser powers; (b) and (c) were observed under the 30% and 15% IR power of (a), respectively. (d)–(f) Simulated spectra (stick diagram) for three conformers obtained at the HF/6-31G(d,p) level calculation; (d) Conformer I, (e) Conformer II, and (f) Conformer III. The vibrational frequencies are multiplied by a factor of 0.8785.

isomers which are energy optimized at the HF/6-31G(d,p) level. In this level calculation, the frequency gap between the hydrogen-bonded OH and the antisymmetric stretch of H_2O is narrower than the observed one. The disagreement may be due to the insufficient basis set of the calculation level. However, even at this level calculation, it is seen that the simulated spectrum of Conformer I shows a good agreement with the observed one with respect of the intensity distribution and the relative positions. As was described above, the reason for many more bands in the observed spectrum than the simulated ones is due to the appearances of the combination bands between the OH stretch and the intermolecular vibrations and of other bands which borrowed their intensities through the Fermi-resonance. Either one of the simulated spectrum of Conformers II [Fig. 7(c)] and III [Fig. 7(d)] does not agree with the observed one for the hydrogen-bonded alcoholic OH of BzA and symmetric stretch bands of the H_2O site. Thus we conclude that the observed BzA–$(H_2O)_2$ cluster corresponds to the *gauche* form cluster of Conformer I.

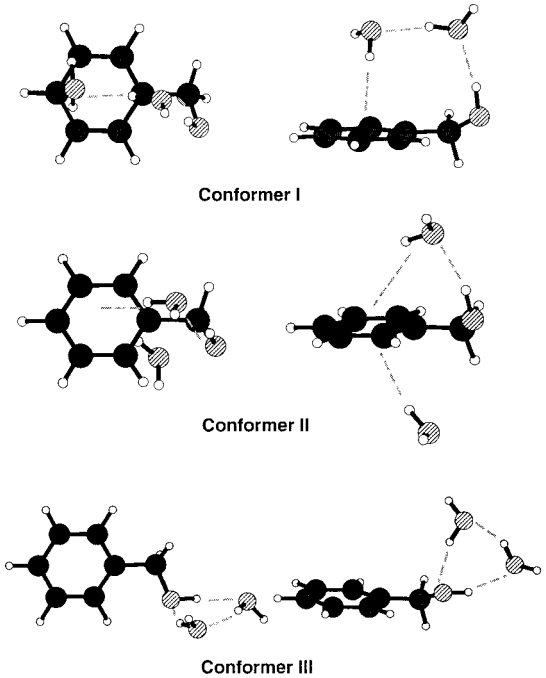

FIG. 6. Energy optimized structures for BzA–$(H_2O)_2$ at the HF/6-31G(d,p) level. Conformer I (left: top view, right: side view): the minimum energy *gauche*-type ring conformer, Conformer II (left: top view, right: side view): higher energy *gauche*-type conformer, and Conformer III (left: top view, right: side view): planar type conformer. Possible hydrogen bondings are shown with broken lines.

D. Benzyl alcohol–$(H_2O)_3$

As shown in Fig. 1(b), the band due to BzA–$(H_2O)_3$ is located at the +192 cm^{-1} higher frequency side of band *A* of bare BzA. The FDIR spectrum of BzA–$(H_2O)_3$ is shown in Fig. 3(c). The aromatic CH stretching bands at 3000–3100 cm^{-1} are again very similar to those of BzA–H_2O and BzA–$(H_2O)_2$, representing that the CH oscillators at this region are not so affected upon the further cluster formation

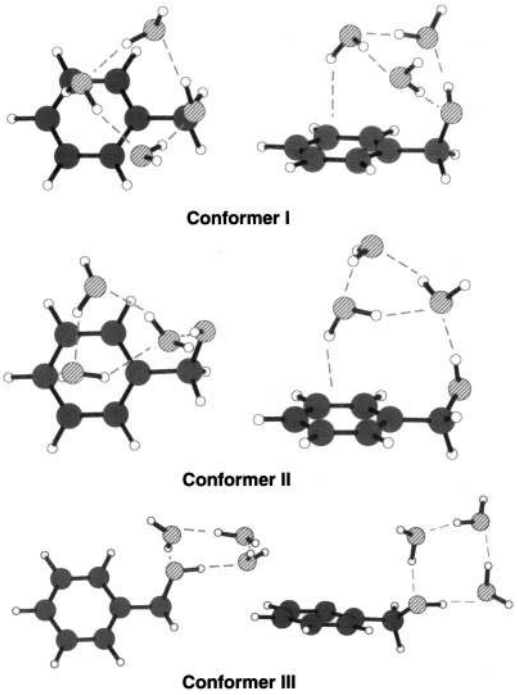

FIG. 8. Energy optimized structures for BzA–$(H_2O)_3$ at the HF/6-31G(d,p) level. Conformer I (left: top view, right: side view): minimum energy *gauche*-type conformer, and Conformer II (left: top view, right: side view): higher energy gauche-type conformer. Conformer III (left: top view, right: side view) represents the planar type higher energy form obtained at the HF/6-31G level. This structure is not obtained as a stable form at the HF/6-31G(d,p) level. Possible hydrogen bondings are shown with broken lines.

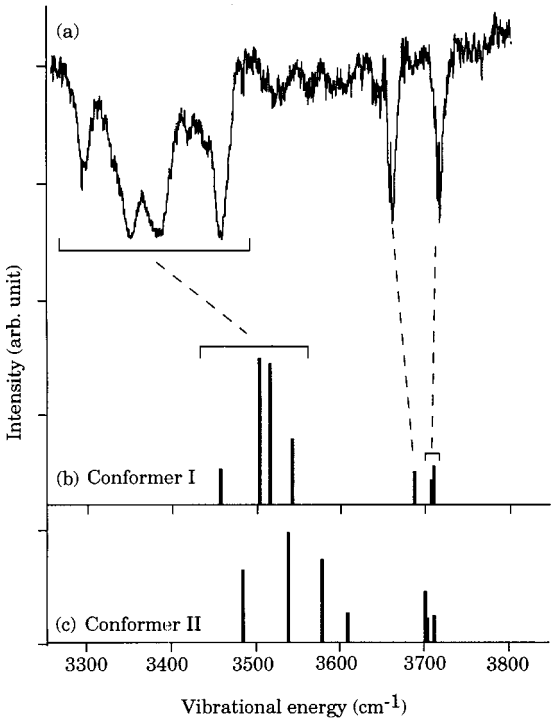

FIG. 9. Comparison of (a) the observed FDIR spectrum of the OH stretching bands of BzA–$(H_2O)_3$ with the simulated spectra (stick diagram) for the two conformers obtained at the HF/6-31G(d,p) level calculation; (b) Conformer I and (c) Conformer II. The height of the bars represents the absorption intensity. The vibrational frequencies are multiplied by a factor of 0.8785.

with H_2O. On the other hand, the aliphatic CH stretch vibrations show much larger frequency shifts. This is also the evidence that the H_2O molecule(s) is hydrogen-bonded to the alcoholic OH group of BzA. The overtone of the OH bending mode is observed at 3208 cm^{-1} similar to that of BzA–$(H_2O)_2$. Other bands appeared at higher than ~3300 cm^{-1} are due to OH stretching vibrations. The highest frequency OH band at 3717 cm^{-1} is due to the antisymmetric stretching mode of the H_2O sites, while the band at 3661 cm^{-1} is characteristic of the π-type hydrogen-bonded OH stretching vibration. The similar π-type hydrogen-bonded OH band is also observed in the benzene–$(H_2O)_3$ clusters.[42] The broad four bands in the 3300–3500 cm^{-1} region are assigned to the σ-type hydrogen-bonded alcoholic OH stretching mode, and symmetric stretching modes of H_2O molecules. It should be noted that there is a large frequency gap between the σ-type hydrogen-bonded OH stretches and the antisymmetric OH stretch bands. This is the typical spectral pattern of the ring-form hydrogen-bonded clusters, which have been demonstrated in the ring-form phenol–$(H_2O)_n$ and 2-naphthol–$(H_2O)_n$ clusters.[38,41]

Figure 8 shows the stable conformers obtained by the *ab initio* calculations at the HF/6-31G(d,p) level. The vibrational frequencies and the IR intensities of the OH stretch bands and the stabilization energies of each conformer are listed in Table II. As seen in the figure, all the low energy conformers exhibit ring-form hydrogen bonding networks. Conformer I is the minimum energy *gauche*-type isomer, in which three H_2O molecules and the alcoholic OH group form a hydrogen-bonded ring. In addition, the OH group of H_2O at the opposite side of the alcoholic OH is hydrogen bonded to π-electrons of the phenyl plane. Though Conformer II is also the *gauche*-type isomer, three H_2O molecules themselves form a ring-type trimer, and the trimer is hydrogen-bonded to the alcoholic OH group and the phenyl plane. Conformer III is the planar type isomer, in which the alcoholic OH group and three H_2O molecules form a ring of hydrogen bonds without making an extra hydrogen bond to the phenyl ring. Although the HF/6-31G level calculation suggested Conformer III to be stable, it was found to be an unstable structure at the HF/6-31G(d,p) level.

The simulated spectra of Conformers I and II are presented in Figs. 9(b) and 9(c), respectively, being compared with the observed FDIR spectrum. Similar to the case of BzA–$(H_2O)_2$, the frequency gap between the hydrogen-bonded OH stretch bands and the antisymmetric stretch bands of H_2O of the simulated spectra is narrower than that observed. In addition, since the simulated two spectra are very similar to each other, it is very difficult to predict the probable conformer only from the IR spectra. However, the simulated spectrum of Conformer I reproduces the characteristic feature of the observed spectrum better than that of Conformer II with respect of the intensity distribution and the position of OH bands. In addition, the calculated binding energy of Conformer I is 1048 cm^{-1} lower than that of Conformer II at the HF/6-31G(d,p) level. Thus, we conclude that the probable structure of BzA–$(H_2O)_3$ in the jet is Con-

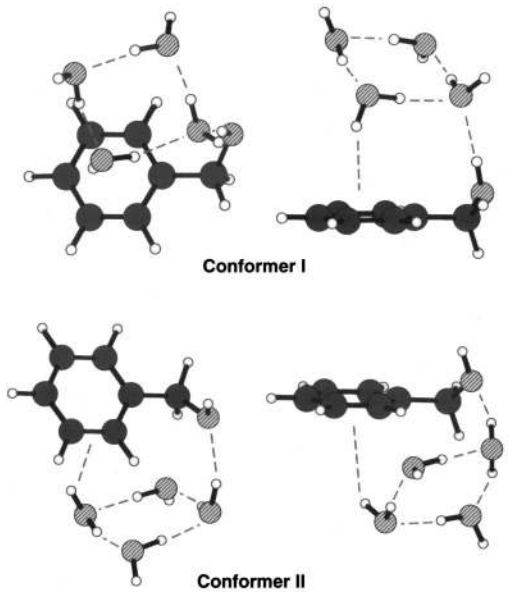

FIG. 10. Energy optimized structures for BzA–$(H_2O)_4$ obtained at the HF/6-31G(d,p) level calculation. Conformer I (left: top view, right: side view): minimum energy *gauche*-type conformer, and Conformer II (left: top view, right: side view): higher energy *gauche*-type conformer. Possible hydrogen bondings are shown with broken lines.

former I, where the three H_2O molecules and the alcoholic OH group make a hydrogen-bonded ring and the whole ring is lying above the phenyl plane with a weak π-hydrogen bond.

E. Benzyl alcohol–$(H_2O)_4$

As shown in Fig. 1(b), the electronic transition of BzA–$(H_2O)_4$ appears at $+150$ cm^{-1} higher frequency side of A band of bare BzA. The observed FDIR spectrum of BzA–$(H_2O)_4$ is shown in Fig. 3(d). The aromatic CH stretching vibrations occurring around 3000–3100 cm^{-1} show the similar spectrum to those of the smaller size clusters. Broad and congested bands in the region of 3200–3450 cm^{-1} are due to σ-type hydrogen-bonded OH stretch vibrations of the water sites and the alcoholic OH group. The overtone band of the OH bending vibration of H_2O at $\sim$3200 cm^{-1} is overlapped with the hydrogen-bonded OH stretching bands. The prominent band at 3653 cm^{-1} band is due to the π-type hydrogen-bonded OH stretch and the bands at $\sim$3720 cm^{-1} correspond to the antisymmetric stretching modes of the H_2O site. The large gap between the σ-type hydrogen-bonded OH stretch bands and the π-type OH stretch or the antisymmetric OH stretch bands of H_2O also suggests the ring-form structure for this cluster.

In Fig. 10, the two stable structures calculated at the HF/6-31G(d,p) level are shown, and the simulated IR frequencies and intensities of the OH stretch bands and the binding energies for each conformer are also given in Table II. As seen in the figure, BzA takes a *gauche* form in both conformers. In these conformers, four H_2O molecules form a ring-form tetramer, which is lying above the phenyl plane. The tetramer is hydrogen-bonded to the alcoholic OH as a proton acceptor in Conformer I, and a donor in Conformer II and the other H_2O is hydrogen-bonded to π-electrons of the phenyl plane.

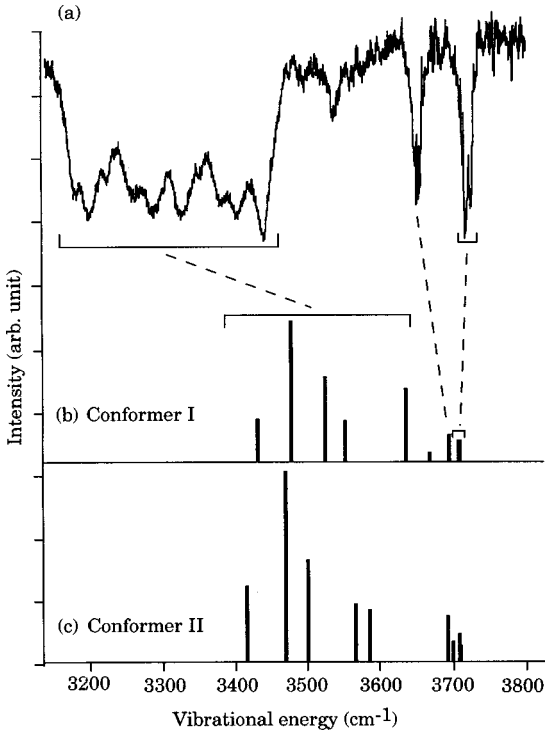

FIG. 11. Comparison of (a) the observed FDIR spectrum of the OH stretching bands of BzA–$(H_2O)_4$ with the simulated spectra (stick diagram) for the two conformers at the HF/6-31G(d,p) level calculation; (b) Conformer I, and (c) Conformer II. The vibrational frequencies are multiplied by a factor of 0.8785.

The simulated spectra for Conformers I and II are presented in Figs. 11(b) and 11(c), respectively. The simulated spectra for the two conformers are very similar with each other, and the difference of their binding energies are is very small, so that the unambiguous discrimination of an irrelevant conformer is difficult at this calculation level. However, in Conformer II it is noticed that the OH group of the alcoholic site acts as a proton acceptor as described above. In all smaller size stable conformers of BzA–$(H_2O)_n$, the alcoholic OH group is involved as a proton donor in the hydrogen-bonding network with H_2O molecules. From the similarity, Conformer I would be the probable structure for the species observed in the jet.

IV. CONCLUSION

A series of spectroscopic work for the OH stretching vibrations of benzyl alcohol and its hydrogen-bonded clusters with water have been performed by IR-UV double resonance spectroscopy in supersonic jets. It was found that for bare molecule the nonhydrogen-bonded ''planar'' form is the dominant species in the jet. On the other hand, the dominant species becomes the ''*gauche*'' conformation in all the clusters with water. In these clusters, water molecules tend to form a ring-type hydrogen-bonding network involving the alcoholic OH group and the whole ring is bound to the phenyl plane through the π-type hydrogen bonding.

ACKNOWLEDGMENTS

N.G. would like to express thank to JSPS for providing fellowship. N.G. also wishes to mention all lab mates (especially Dr. A. Fujii, Dr. Shin Sato, Dr. H. Ishikawa, Dr. T. Maeyama, and Dr. Y. Matsuda) for their constant help during experiments. This work is partially supported by the Grant-in-Aids for Scientific Research (No. 10440165) by the Ministry of Education, Science, Sports, and Culture, Japan. T.E. also acknowledges the support from the Kurata Foundation.

[1] P. M. Felker, P. M. Maxton, and M. W. Schaeffer, Chem. Rev. **94**, 1787 (1994).
[2] Q. Y. Shang and E. R. Bernstein, Chem. Rev. **94**, 2015 (1994).
[3] T. Ebata, A. Fujii, and N. Mikami, Int. Rev. Phys. Chem. **17**, 331 (1998).
[4] J. A. Odutola and T. R. Dyke, J. Chem. Phys. **72**, 5062 (1980).
[5] G. T. Fraser, Int. Rev. Phys. Chem. **10**, 189 (1991).
[6] E. Zwart, J. J. Ter Meulen, W. L. Meerts, and L. H. Coudert, J. Mol. Spectrosc. **147**, 27 (1991).
[7] L. H. Coudert, F. J. Lovas, R. D. Suenram, and J. T. Hougen, J. Chem. Phys. **87**, 6290 (1987).
[8] Z. S. Huang and R. E. Miller, J. Chem. Phys. **91**, 6613 (1989).
[9] K. L. Busarow, R. C. Cohen, G. A. Blake, K. B. Laughlin, Y. T. Lee, and R. J. Saykally, J. Chem. Phys. **90**, 3937 (1989).
[10] N. Pugliano, J. D. Cruzan, J. G. Loeser, and R. J. Saykally, J. Chem. Phys. **98**, 6600 (1993).
[11] F. Huisken, M. Kaloudis, and A. Kulcke, J. Chem. Phys. **104**, 17 (1996).
[12] K. Liu, J. G. Loeser, M. J. Elrod, B. C. Host, J. A. Rzepiela, N. Pugliano, and R. J.Saykally, J. Phys. Chem A. **116**, 3507 (1994).
[13] K. Liu, J. D. Cruzan, and R. J. Saykally, Science **271**, 929 (1996).
[14] K. Liu, M. G. Brown, and R. J. Saykally, J. Phys. Chem. A **101**, 8995 (1997).
[15] K. Liu, M. G. Brown, J. D. Cruzan, and R. J. Saykally, J. Phys. Chem. A **101**, 9011 (1997).
[16] J. D. Cruzan, M. K. Viant, M. G. Brown, and R. J. Saykally, J. Phys. Chem. A **101**, 9023 (1997).
[17] M. K. Viant, J. D. Cruzan, D. D. Licus, M. G. Brown, K. Liu, and R. J. Saykally, J. Phys. Chem. A **101**, 9032 (1997).
[18] C. Lee, H. Chen, and G. Fitzgerald, J. Chem. Phys. **102**, 1266 (1995).
[19] J. O. Jensen, P. N. Krishnan, and L. A. Burke, Chem. Phys. Lett. **246**, 13 (1995).
[20] K. S. Kim, B. J. Mhin, S. J. Lee, and K. S. Kim, Chem. Phys. Lett. **219**, 243 (1994).
[21] K. S. Kim, M. Dupuis, G. C. Lie, and E. Clementi, Chem. Phys. Lett. **131**, 451 (1986).
[22] C. J. Tsai and K. D. Jordan, J. Chem. Phys. **95**, 3850 (1991).
[23] C. J. Tsai and K. D. Jordan, J. Phys. Chem. **97**, 5208 (1993).
[24] J. Wales and I. Ohmine, J. Chem. Phys. **98**, 7257 (1993).
[25] K. Laasonen, M. Parinello, R. Car, C. Lee, and D. Vanderbilt, Chem. Phys. Lett. **207**, 208 (1992).
[26] S. S. Xantheas J. Chem. Phys. **100**, 7523 (1994); **102**, 4505 (995).
[27] N. Gonohe, H. Abe, N. Mikami, and M. Ito, J. Phys. Chem. **89**, 3642 (1985).
[28] R. J. Lipert and S. D. Colson, J. Phys. Chem. **94**, 2358 (1990).
[29] M. F. Hineman, D. F. Kellay, and E. R. Bernstein, J. Chem. Phys. **99**, 4533 (1993).
[30] R. J. Stanley and A. W. Castleman, Jr., J. Chem. Phys. **98**, 796 (1993).
[31] H. S. Gutowsky, T. Emilsson, and E. Arunan, J. Chem. Phys. **99**, 4883 (1993).
[32] O. Dopfer, G. Reiser, K. Muller-Dethlefs, E. W. Schlag, and S. D. Colson, J. Chem. Phys. **101**, 974 (1994).
[33] R. N. Pribble and T. S. Zwier, Science **265**, 75 (1994).
[34] P. M. Maxton, M. W. Schaeffer, and P. M. Felker, Chem. Phys. Lett. **241**, 603 (1995).
[35] T. Ebata, T. Watanabe, and N. Mikami, J. Phys. Chem. **99**, 5761 (1995).
[36] R. M. Helm, H. P. Vogel, and H. J. Neusser, J. Chem. Phys. **108**, 4496 (1997).
[37] M. Schmitt, Ch. Jacoby, and Kleinermanns, J. Chem. Phys. **108**, 4486 (1997).
[38] T. Watanabe, T. Ebata, S. Tanabe, and N. Mikami, J. Chem. Phys. **105**, 408 (1996).
[39] T. Ebata, N. Mizuochi, T. Watanabe, and N. Mikami, J. Phys. Chem. **100**, 546 (1996).
[40] A. Mitsuzuka, A. Fujii, T. Ebata, and N. Mikami, J. Chem. Phys. **105**, 2618 (1996).
[41] Y. Matsumoto, T. Ebata, and N. Mikami, J. Chem. Phys. **109**, 6303 (1998).
[42] R. N. Pribble and T. S. Zwier, Faraday Discuss. **97**, 229 (1994).
[43] R. N. Pribble, A. W. Garret, K. Haber, and T. S. Zwier, J. Chem. Phys. **103**, 603 (1995).
[44] S. Y. Fredericks, K. D. Jordan, and T. S. Zwier, J. Phys. Chem. **100**, 7810 (1996).
[45] C. J. Gruenloh, J. R. Carney, F. C. Hagemeister, C. A. Arrington, T. S. Zwier, S. Y. Fredericks, J. T. Wood III, and K. D. Jordan, J. Chem. Phys. **109**, 6601 (1998).
[46] S. Knof, H. Strassmair, J. Engel, M. Rothe, and K. D. Steffen, Biopolymers **11**, 731 (1972).
[47] S. Li and E. R. Bernstein, J. Chem. Phys. **97**, 7383 (1992).
[48] M. I. Matheu, R. Echarri, and S. Castillon, Tetrahedron Lett. **34**, 2361 (1993).
[49] M. Faubel, B. Steiner, and J. P. Toennies, J. Chem. Phys. **106**, 9013 (1997).
[50] N. Guchhait, T. Ebata, and N. Mikami, J. Am. Chem. Soc. **121**, 5705 (1999).
[51] M. J. Frisch, G. H. Trucks, H. B. Schlegel, P. M. W. Gill, B. J. Johnson, M. A. Robb, J. R. Cheeseman, T. Keith, G. A. Petersson, J. A. Montgomery, K. Raghavachari, M. A. Al-Laham, V. G. Zakrzewski, J. V. Ortiz, J. B. Foresman, J. Cioslowski, B. B. Stefanov, A. Nanayakkara, M. Challacombe, C. Y. Peng, P. Y. Ayala, W. Chen, M. W. Wong, J. L. Andres, E. S. Replogle, R. Gomperts, R. L. Martin, D. J. Fox, J. S. Binkley, D. J. Defrees, J. Baker, J. P. Stewart, M. Head-Gordon, C. Gonzalz, and J. A. Pople, GAUSSIAN 94, Gaussian, Inc., Pittsburgh, Pennsylvama, 1995.
[52] M. Oki and H. Iwamura, Bull. Chem. Soc. Jpn. **32**, 950 (1959).
[53] M. Oki and H. Iwamura, Bull. Chem. Soc. Jpn. **32**, 955 (1959).
[54] M. Oki and H. Iwamura, Bull. Chem. Soc. Jpn. **32**, 1135 (1959).
[55] W. J. Hehre, L. Radom, and J. A. Pople, J. Am. Chem. Soc. **94**, 1496 (1972).
[56] M. Ito and M. Hirota, Bull. Chem. Soc. Jpn. **54**, 2093 (1981).
[57] H. S. Im, E. R. Bernstein, H. V. Secor, and J. I. Seeman, J. Am. Chem. Soc. **113**, 4422 (1991).
[58] G. Herzberg, *Molecular Spectra and Molecular Structure II, Infrared and Raman Spectra of Polyatomic Molecules* (Van Nostrand Reinhold, New York, 1945).